Vertex finding performance studies for the Phase II CMS Level-1 Trigger

Silviu Marian Udrescu

September 2017

1 Abstract

At the HL-LHC, a significant increase in the luminosity delivered to CMS will result in a pileup per bunch crossing of 140-200. This provides a difficult environment to obtain reliable physics results and keep trigger rates manageable. In order to mitigate this problem, tracker information will be used, for the first time, at the Level-1 (L1) trigger. This will allow the primary vertex reconstruction at L1. In this report, an investigation into the vertex finding performance of a potential algorithm is presented. The vertex finding efficiency was measured as a function of several variables, such as the percentage of tracks associated to the primary vertex within the barrel and the p_T of the tracks. The efficiency was found to not depend significantly on the pileup for the samples analyzed, however, a strong dependence was observed on the number of tracks associated with the primary vertex.

2 Introduction

The Large Hadron Collider (LHC) is expected to be upgraded (Phase II upgrade) around 2024 in order to increase the peak luminosity to $5 - 7.5 \times 10^{34}$ cm^{-2}s^{-1} [1]. This would correspond to approximately $140 - 200$ proton-proton interactions, called pileup (PU), per bunch crossing at a frequency of 40 MHz [2]. With a total integrated luminosity of 3000 fb^{-1}, the High-Luminosity LHC (HL-LHC) will allow searches for rare processes, high precision Higgs measurements and increase the chance of finding new particles with low cross-section. However, this high luminosity environment will pose numerous challenges related to pileup mitigation and vertex reconstruction.

3 Tracker

The Compact Muon Solenoid (CMS) is a general purpose detector at the LHC, whose main feature is a superconducting solenoid able to provide a magnetic field of 3.8 T [3]. Inside the solenoid volume, starting out from the interaction point, the subdetectors composing the experiment are: the silicon tracker, the electromagnetic and hadronic calorimeters, while outside the solenoid there are gas-ionizing detectors, used as muon detectors [2]. In order to obtain reliable physiscs results, the trajectories of the charged particles, coming from the collision points, as well as from the secondary vertices, must be reconstructed with a high precision [4]. This task is accomplished by the silicon tracker system.

The tracking system is composed of a silicon pixel inner tracker and a larger strip outer tracker [4]. The inner tracker covers a pseudo-rapidity range $|\eta| < 2.5$, containing 3 layers in the barrel and 2 endcap disks. The outer tracker is divided intro 3 regions: Tracker Inner Barrel and Disk (TIB/TID), located in the region $20 < r < 55$ cm, $|z| < 118$ cm, the Tracker Outer Barrel (TOB) with $55 < r < 116$ cm and $|z| = 118$ cm, and between $22.5 < r < 113.5$ cm, $124 < |z| < 282$ cm there is the end cap area called Tracker EndCaps (TEC). With an average hit rate of 1 MHz in the inner region and 3 kHz in the outermost one, the tracker has high granularity in order to keep the occupancy below 1% per sensor per bunch crossing, which is required for proper track and vertex reconstruction.

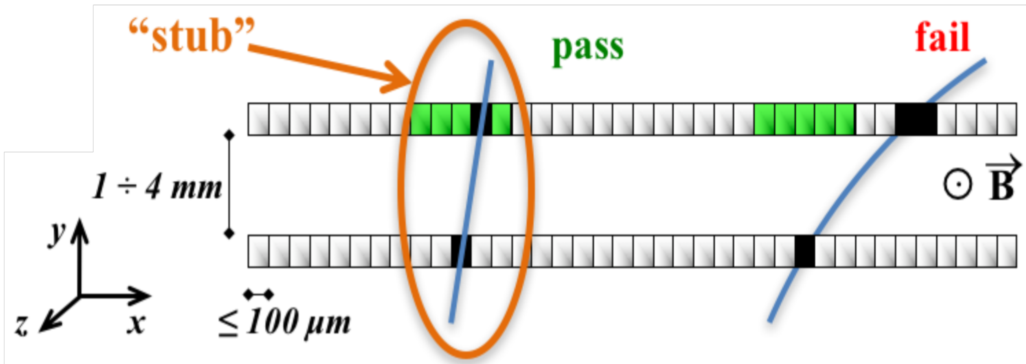

Figure 1: Closely spaced sensor layers allow the discrimination of the tracks p_T, based on their bending in the magnetic field [2].

4 Trigger

Currently, the pileup at LHC is about 40-55, at a rate of one bunch crossing every 25 ns [4]. This event rate of 40 MHz needs to be reduced considerably in order for the full detector data to be stored to disk. This rate reduction is done in 2 steps through the CMS trigger system. The first, the Level-1 (L1) trigger, is made up of custom-made electronics and is able to reduce the rate to approximately 100 kHz, while the second, the High Level Trigger (HLT), further reduces it to a rate of $\mathcal{O}(1)$ kHz. The L1 trigger uses segmented information from muon and calorimeter systems. When an event is accepted, the data is passed to the Front-end Readout Link (FRL) boards representing the interface to the Data Acquizion (DAQ) system and from there to the HLT. The L1 trigger has an intrinsic flexibility due to the implementation of algorithms in programmable FPGA's, allowing for general algorithm improvements, as well as adjustment necessary for increasing luminosity and pileup. The HTL is implemented in software, running on a computer farm of commercial CPUs known as the Event Filter Farm (EVF). It is composed of a series of reconstruction and filtering algorithms arranged in increasing complexity aiming for the lowest possible CPU running time.

5 Phase 2 Upgrade

At the HL-LHC, the pileup will increase to 140-200 [2]. This will require the replacement of the CMS tracker in order to increase the granularity, maintain a high track reconstruction efficiency and a low mis-identification rate. As Higgs boson studies will still be a main focus for the CMS program for Phase II, p_T thresholds must be kept low at the L1 trigger [4]. Therefore, in order to keep trigger rates manageable, the L1 trigger efficiencies must be improved. Some of this improvement will come from using tracker information in the L1 trigger to keep the L1 accept rate below 750 kHz. This new information in the L1 trigger requires the implementation of a new module design in the outer tracker, called the "p_T module", which consists of two sensors separated by several millimeters allowing the measurement of the charged particles p_T based on the curvature of the track inside the magnetic field (Figure 1) [2,4].

Tracks with a p_T above $2-3$GeV are readout by the front-end electronics in the form of stubs, which are the tracker trigger primitives that are sent to the track trigger processor as input to the track finding and fitting algorithms. Only selecting tracks with a p_T above $2-3$GeV gives a rate reduction of data coming to the track trigger of 10 to 100.

There are two types of p_T modules: pixel-strip modules (PS) and strip-strip modules (2S). PS modules have an active area of 4.69cm $\times$9.60cm and cover the range $20 < r < 60$cm. They contain a lower silicon pixel sensor and an upper silicon strip sensor, with a pitch along the beam axis z of 1.47mm for the pixels and 2.35cm for the strips and a pitch of 100μm in r-φ plane. The 2S modules will cover $r > 60$cm, with an active area of 10.05cm $\times$9.14cm and the two sensors will have a pitch of 5.03cm in the z direction and 90μ in r-φ. The module placement inside the outer trigger is presented in Figure 2.

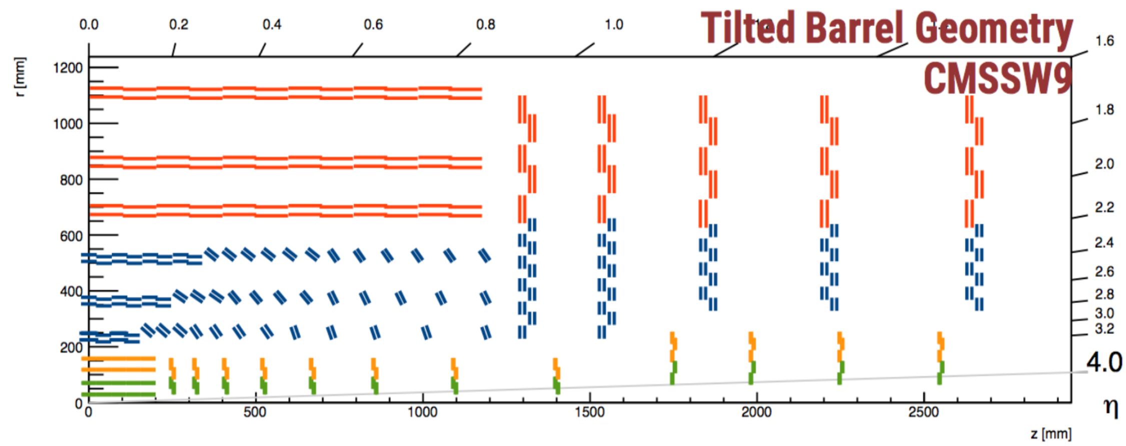

Figure 2: A quadrant of the new outer tracker layer, presenting the location of the PS (blue) and 2S (red) modules [2].

6 Track Reconstruction

In order to be used for online analysis, the L1 Track Trigger must be able to reconstruct tracks out of stubs with a $p_T > 3$GeV and with a high efficiency in 4μs [2,4]. To study the performance of the L1 Track Trigger, Monte Carlo (MC) data is used to simulate various physics processes. Several cuts have to be imposed on the generated MC truth tracks and emulated L1 tracks. An L1 track is considered to be matched with a truth track when it contains four stubs produced by the same truth particle. The cuts applied to the tracks can be seen in Table 1. In order to characterize the L1 tracking performance, 3 parameters are investigated: efficiency, resolution and the output rate of tracks [4]. The first one is defined as the ratio of the number of L1 tracks matching a truth track, to the number of truth tracks. Resolution is defined as the interval where 90% of the tracks are within the residual distribution $x = p_{Matched} - p_{Truth}$, for a given parameter p. The output rate represents the average number of L1 tracks in each event. A Hough Transform (HT), which is a method used for detecting geometric features from digital images, implemented in the FPGA firmware, will be used in order to identify the tracks out of the set of stubs [2]. Then, Linear Regression will be employed for the fitting and filtering of the track candidates produced by the HT.

Truth Particles	$p_T > 3$GeV ≥ 4 stubs in ≥ 4 layers $\lvert\eta\rvert \leq 2.4$ $\lvert z_0\rvert \leq 30$ cm $d_{xy} < 1$ cm
L_1 Tracks	$\lvert\eta\rvert \leq 2.4$ $z_0 \leq 30$ cm ≥ 4 stubs in ≥ 4 layers
Matched Tracks	same as L_1 Tracks ≥ 4 stubs matched with a single truth particle

Table 1: Cuts imposed on Truth, L1 and Matched tracks[4].

7 Vertex Reconstruction

With the addition of the track information, primary vertex (PV) reconstruction is now also possible at L1 [5]. This has potential to significantly mitigate the increased rate due to pileup. The PV finding algorithm used was DBSCAN (Density-Based Spatial Clustering of Applications with Noise) [6]. Previous studies have shown that it is currently the best compromise between feasibility of hardware implementation, and reconstruction efficiency [5]. The L1 tracks considered for the algorithm must have a p_T above a configurable threshold. They must have stubs in at least four different tracker layers and a χ^2 per degrees of freedom, above 20. The main benefits of this algorithm are that it doesn't require sorting of tracks and is robust against outliers [7]. DBSCAN groups together tracks that are within a configurable distance from each other, ϵ and requires that each group has a configurable minimum number of tracks. Also, being a density based algorithm, the result is independent of the shape of the tracks distribution. From the list of vertices returned by the DBSCAN algorithm, the one with the highest total p_T is chosen as the PV if it has a minimum number of tracks associated with it. The PV is considered well reconstructed if it is within a configurable distance from the truth PV. This is called the matching distance d_0 and for this analysis was set to 1mm.

8 Analysis

In this study, the PV reconstruction was characterized by measuring changes in the reconstruction efficiency when various parameters were changed. Several MC samples produced with the event generator PYTHIA, and with the detector response simulated using Delphes were used [7]. The processes studied were: $t\bar{t}$, VBF H $\rightarrow$ invisible (VBF), DoubleGluonGunFlatPt50300 (GG), GluGluHToZZTo4L, QCDPt-15to3000 and VBF H $\rightarrow$ BB. Each sample was generated at a centre-of-mass energy of 14TeV, and for 0, 140 and 200 pileup. Cuts were applied to track parameters and to the properties of the reconstructed PV. The PV reconstruction efficiency is defined in each bin as the ratio between the number of reconstructed PVs and the number of truth PVs in that bin. The PV reconstruction efficiency was found to be strongly dependent on the physics process. Figure 3 shows the efficiency of 3 different processes plotted as a function of the position along z of the truth PV. The efficiency is not found to be strongly dependent on pileup or the z_0 of the PV for the samples shown.

The p_T threshold of the tracks used in the PV reconstruction was set to 3, 5 and 10GeV. The efficiency in bins of the truth PV z_0 is shown in Figure 4. For $t\bar{t}$ and GG, changing the track p_T threshold does not have a significant effect. However, for the VBF sample, between 3 and 10GeV, the efficiency increases by 20%, at all pileups. Due to the fact that there is no strong dependence of the efficiency on the z_0 of the truth PV, the next step was to measure the efficiency in bins of number of truth tracks associated with the PV. It can be seen that the efficiency significantly increases with the number of tracks (Figure 5). When binning in number of tracks with a p_T above 3, 5 and 10GeV, the efficiency increases for PVs with less than 15 tracks associated to them. For the remainder of the

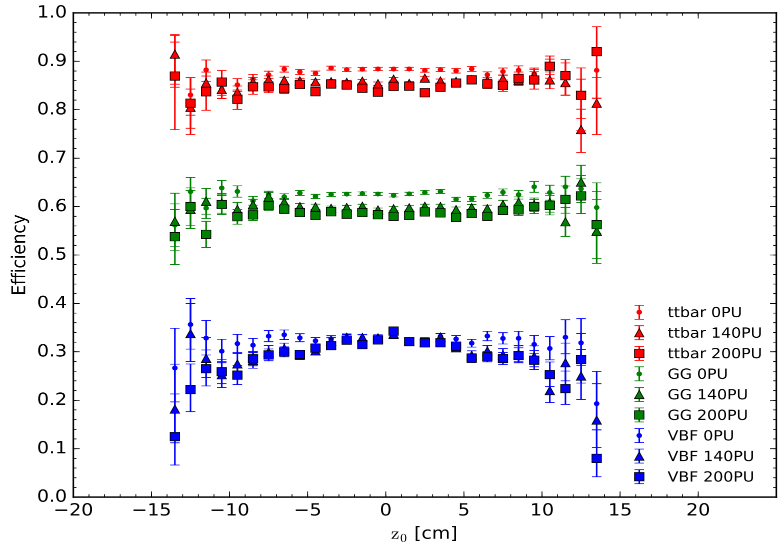

Figure 3: PV reconstruction efficiency of the DBSCAN algorithm for $t\bar{t}$, VBF and GG at 0, 140 and 200 pileup, as a function of the position of the truth vertex.

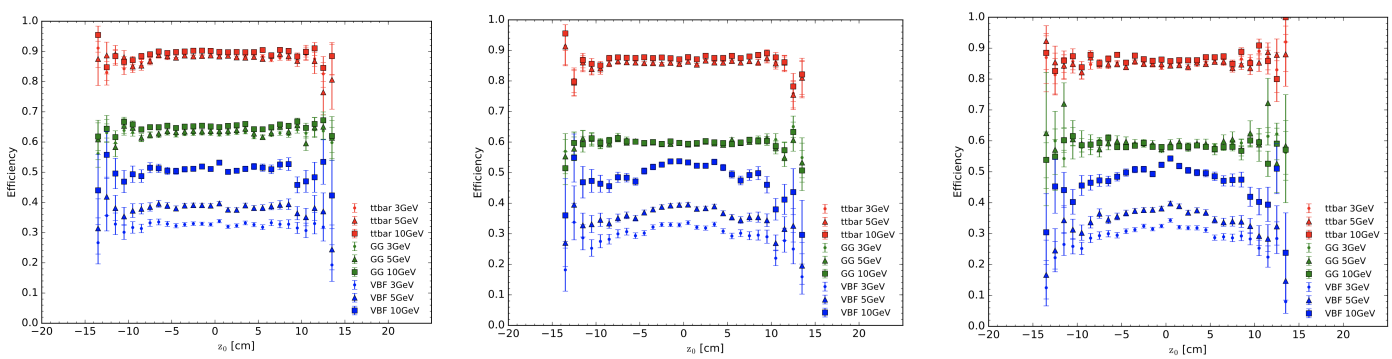

Figure 4: PV reconstruction efficiency of the DBSCAN algorithm for $t\bar{t}$, VBF and GG with differents cuts on the minimum p_T of the tracks used for reconstructions at 0, 140 and 200 PU.

analysis, a 3GeV threshold was applied to the track p_T. Histograms will now only be shown for zero pileup, unless the results for higher pileup are significantly different.

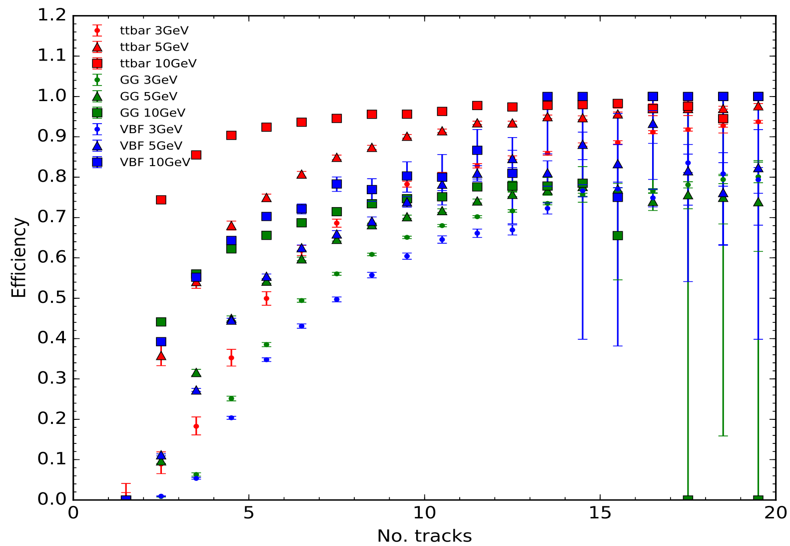

Figure 5: PV reconstruction efficiency of the DBSCAN algorithm as a function of number of tracks associated with the PV, for $t\bar{t}$, VBF and GG with different cuts on the minimum p_T of the tracks used for reconstruction at 0PU.

Next, the percentage of tracks associated with the PV that are located in the barrel was calculated for each vertex. A track is in the barrel if it has $|\eta| < 0.9$. The PV efficiency was then calculated taking into account only vertices that have at least 50% or 90% of the associated tracks in the barrel. The efficiency is significantly increased in all bins for all 3 samples by requiring >50 % of tracks in the barrel (Figure 6). The increase from 50% to 90% improves the efficiency for the $t\bar{t}$ and VBF samples, however this has no significant effect on the efficiency for the GG sample. When applying the cut at 90%, the efficiency for the $t\bar{t}$ and GG samples have the same value, within statistical error, for PVs having 5 or more tracks associated with them. The percentage of PVs that remain after each cut, out of the initial number of vertices, when no cut on the tracks in the barrel is applied is shown in Table 2.

$t\bar{t}$	$t\bar{t}$ 50%	$t\bar{t}$ 90%	VBF	VBF 50%	VBF 90%	GG	GG 50%	GG 90%
100.0%	47.0%	5.2%	100%	26.0%	15.3%	100%	17.3%	16.3%

Table 2: Percentage of remaining primary vertices, after the cuts on the percentage of tracks within the barrel is applied, out of the total number of primary vertices.

The efficiency as a function of the number of layers traversed by a track, and as a function of whether the first layer was hit or not is shown in Figure 7. The reconstruction efficiency is lower for PVs having at least one track with hits in 7 layers, and for PVs with at least one track without a hit in the first tracker layer. The number of events with a track that hits all 7 layers is less than 10% of the total number of tracks in the generated events and close to 0 when the first layer is not hit. This can be seen in Figure 8 for $t\bar{t}$, and similar results are observed for the other samples studied. Therefore, setting a cut on the tracks, such that only tracks that hit the first layer and have hits in <7 layers, increases the efficiency without discarding a significant number of tracks. The results obtained by applying these 2 cuts are shown in Figure 9. For all 3 samples, if these cuts are applied

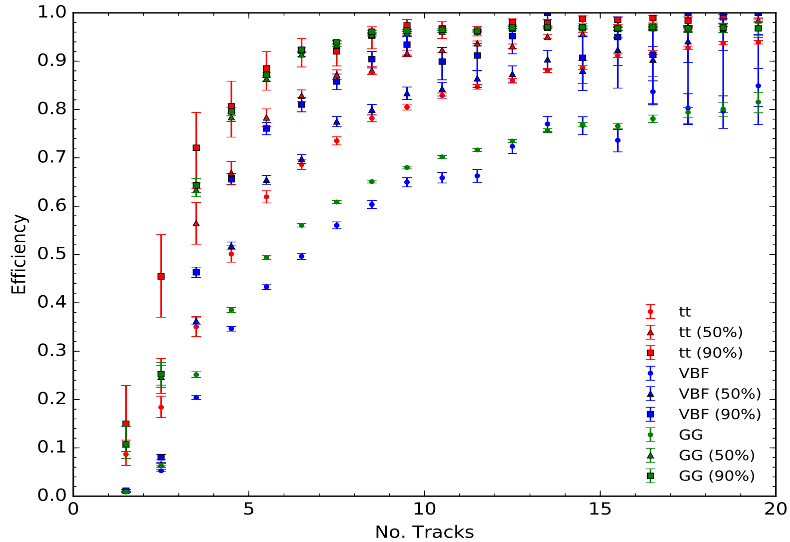

Figure 6: PV reconstruction efficiency of the DBSCAN algorithm for $t\bar{t}$, VBF and GG, for 0,50 and 90% of tracks in the barrel, at 0PU.

after applying the cut on the percentage of tracks within the barrel, the efficiency is not significantly affected for a number of tracks greater than 6.

The other 3 samples, GluGluHToZZTo4L, QCDPt-15to3000 and VBF H $\rightarrow$ BB, were then studied. The results from zero pileup is shown in Figure 10. A similar trend to the previous samples is observed, independent of the initial efficiency of the sample. It can be noticed, however, that the layer cuts have a visible effect on the QCDPt-15to3000 at 14 TeV sample, even for more than 6 tracks.

Sample	$t\bar{t}$	VBF $H \rightarrow inv$	VBF $H \rightarrow BB$	GG	GluGluHToZZTo4l	QCD$_P t15to3000$
Remained events	5.2%	15.3%	9%	16.3%	6.8%	12.6%

Table 3: Percentage of remained PV out of the total number of PVs, after the cuts on the percentage of tracks within the barrel is applied, for all sample.

Sample	$t\bar{t}$	VBF H $\rightarrow$ inv	VBF H $\rightarrow$ BB	GG	GluGluHToZZTo4l	QCD$_P t15to3000$
Remained events	8.5%	18.8%	13.9%	16.3%	13.3%	15.9%

Table 4: Percentage of remained PVs out of the total number of PVs, after the cuts on the percentage of tracks within the barrel and the layer cuts are applied, for all sample.

A comparison of all samples studied is shown in Figure 11, for the 90% cut on the percentage of tracks in the barrel with and without the layer cuts (histograms showing also the 50% cut can be found in the Appendix). For <10 tracks, $t\bar{t}$, GG and GluGluHToZZTo4L have similar efficiency, while VBF, VBF H $\rightarrow$ BB and QCDPt-15to3000 have lower efficiency. However, above 10 tracks, the difference is significantly reduced. A similar trend can be observed for the efficiencies resulting from the cuts on the η and the layer cuts. Table 3 presents the percentage of events that pass the cut requiring 90% of the tracks within the barrel and in Table 4 the percentage is calculated when the layer cuts are used first. This percentage is increased for all samples when the layer cuts are applied,

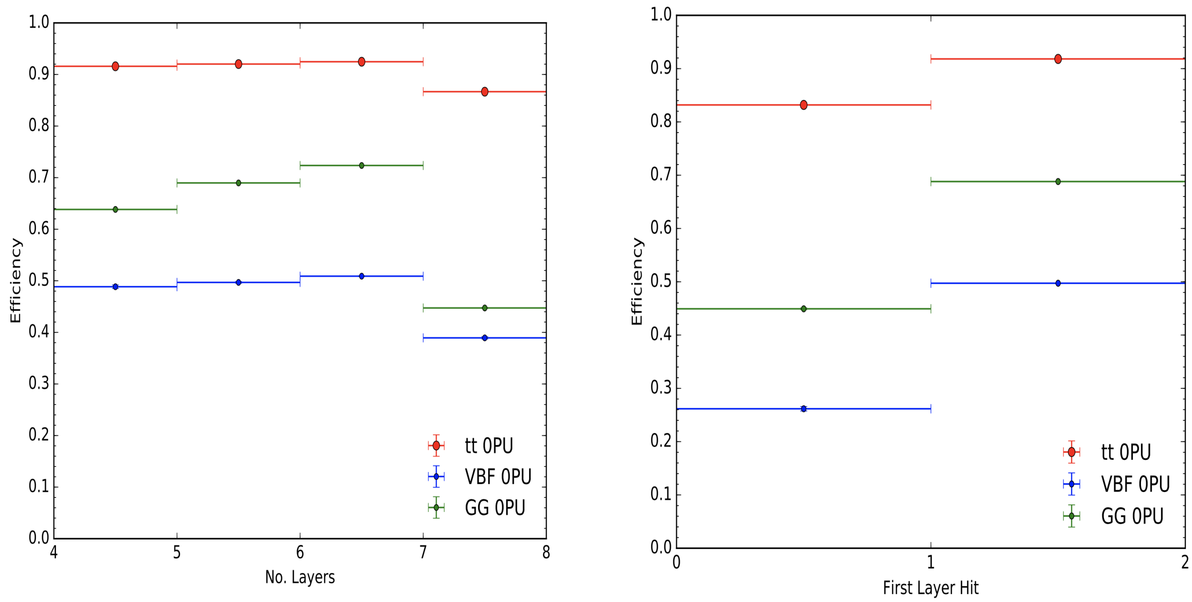

Figure 7: PV reconstruction efficiency of the DBSCAN algorithm for $t\bar{t}$ at 0 pileup as a function of the number of layers hit by tracks associated with that PV (left) and as a function of whether a track hit the first layer (right). 0 = no hit, 1 = hit.

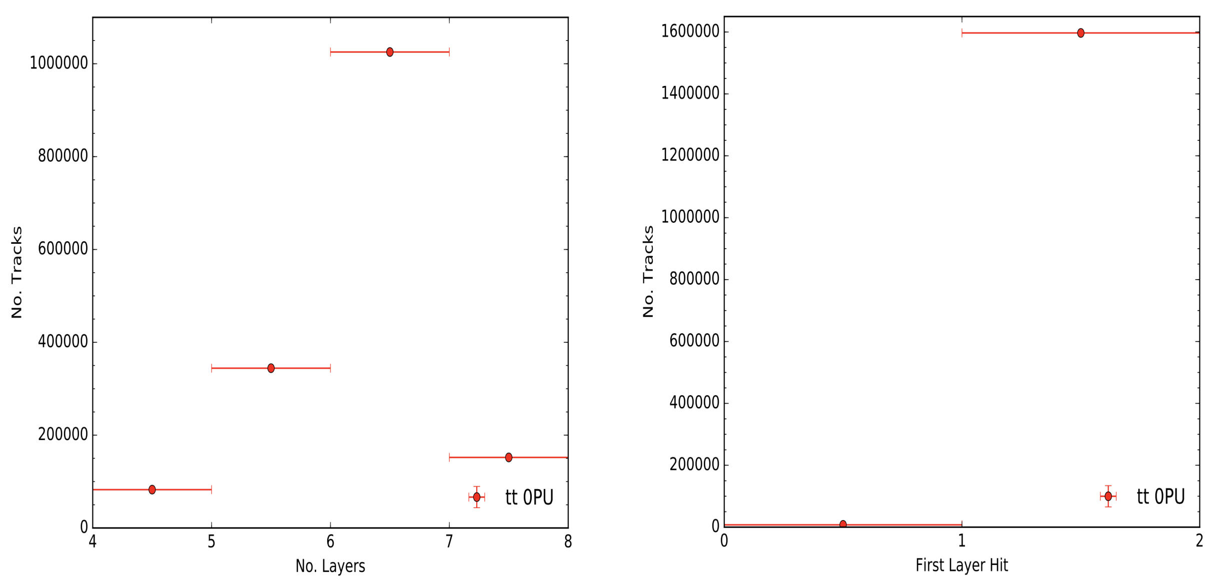

Figure 8: Histograms of the number of tracks associated with the PV, with a certain number of hits in the tracker layers in the simulated events (left) and of the number of tracks with and without a hit in the first layer (right) for the $t\bar{t}$ sample.

suggesting that part of the tracks with 7 hits or without a hit in the first layer are outside the barrel. Thus, even if the layer cuts have no major effect on the efficiency, once the cut on the percentage of tracks within the barrel is applied, they can allow more events to pass the cuts and provide high statistics.

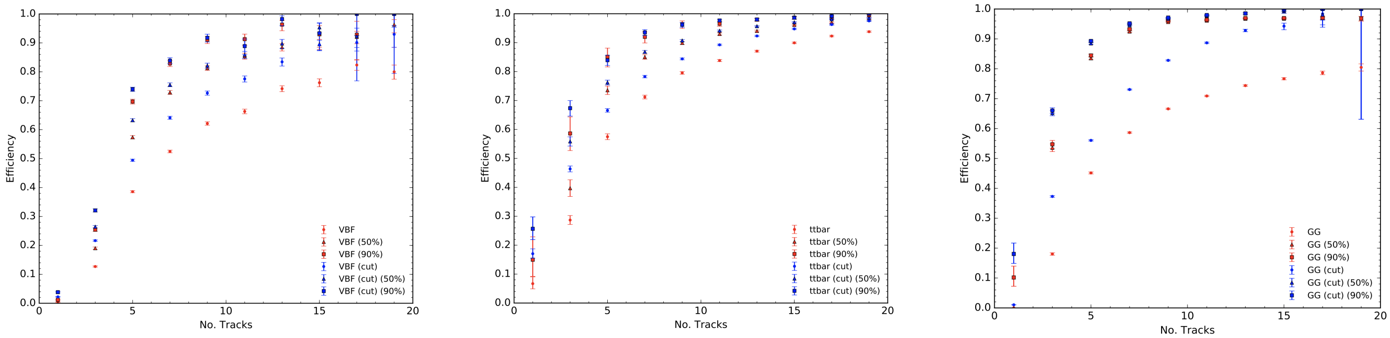

Figure 9: PV reconstruction efficiency of the DBSCAN algorithm for $t\bar{t}$, VBF and GG, with the layers cut and the cut on the 0,50 and 90% of tracks in the barrel at 0PU.

9 Conclusion

In this study, changes in the PV reconstruction efficiency algorithm were investigated by varying several track parameters and PV properties. By increasing the threshold on the p_T of the tracks used for PV reconstruction, from 3 to 5 and then to 10 GeV, an increase in the efficiency was observed for all 3 samples in bins of number of tracks. In the same binning, a significant increase in the efficiency was observed when only the PVs with more than 50% and then 90% of the tracks in the barrel were considered. In this case, the efficiencies from the $t\bar{t}$ and GG samples had similar values for all bins, while VBF was similar only when >10 tracks are associated to the PV. However, this threshold discards a significant number of events, such that the PVs for these events are not taken into account in the calculation of the efficiency. Finally, the cut on the number of tracker layers and the presence of a hit in the first layer showed an increase in the efficiency without discarding a significant number of tracks. When the cut on the percentage of tracks in the barrel is applied, the effect of the layer cuts is no longer significant, however, a larger number of events pass the cuts.

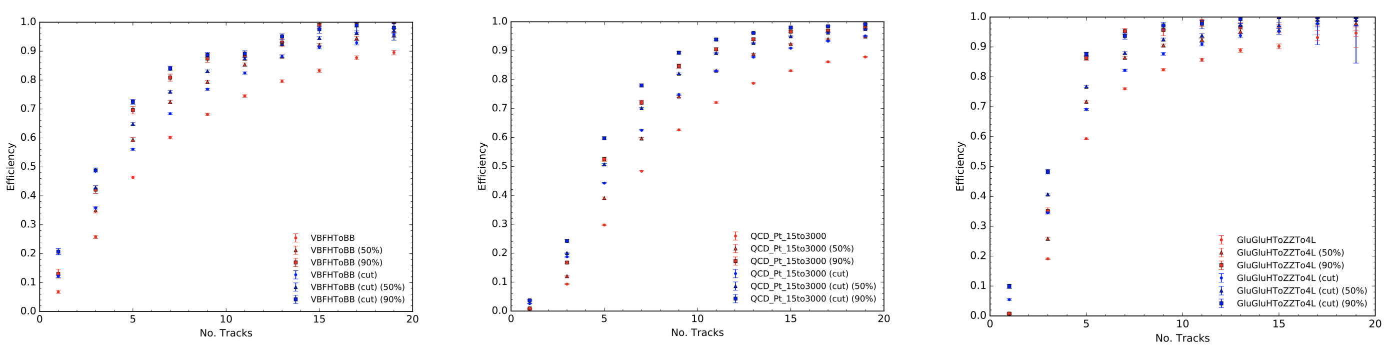

Figure 10: PV reconstruction efficiency of the DBSCAN algorithm for GluGluHToZZTo4L, QCDPt-15to3000 and VBF H $\rightarrow$ BB, with the layers cut and the cuts on 0,50 and 90% of tracks in the barrel at 0PU.

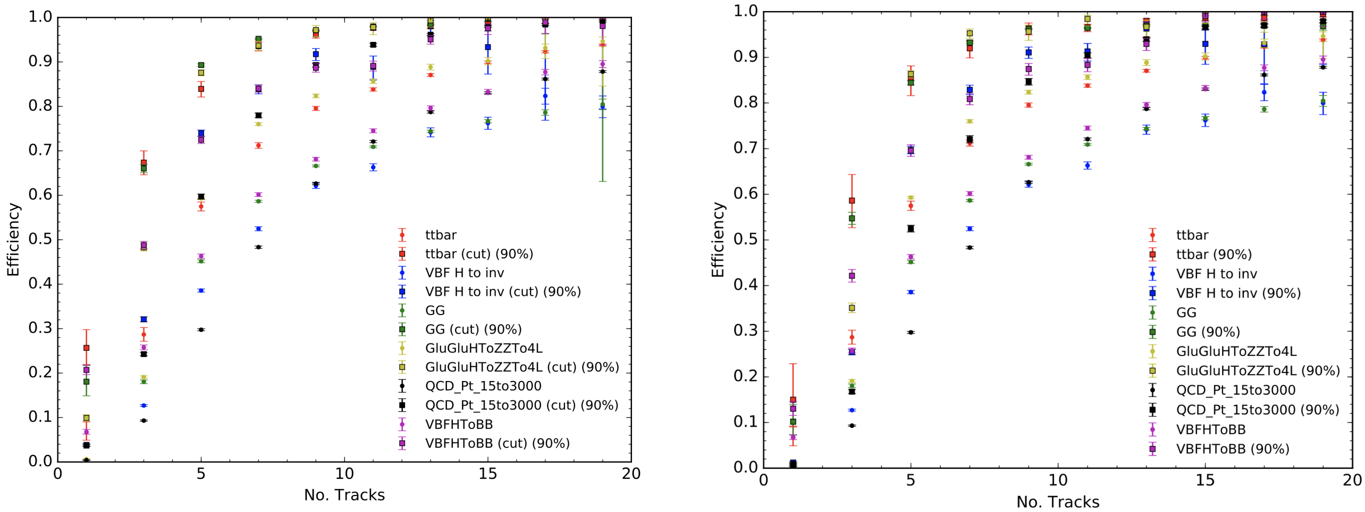

Figure 11: PV reconstruction efficiency of the DBSCAN algorithm for all the considered sample, only with the 90% cut on the percentage of tracks in the barrel (left), and with the 90% cut on the percentage of tracks in the layer and the layers cut, at 0PU.

Further studies will include the characterization of the PV finding efficiency for different values of the matching parameter d_0. Also, the effect on the efficiency of changing the minimum number of layers a track must traverse in order to be included in the PV reconstruction will be studied. These studies will allow a better understanding of the useful properties and parameters needed for PF and PUPPI.

10 Acknowledgements

The author would like to thank Alex Tapper, Emmanuel Perez, Aaron Bundock, Davide Cieri, Antoni Shtipliyski, Tom Williams, Mark Pesaresi and Tom James for the help provided for this project.

11 References

[1] THE CERN LARGE HADRON COLLIDER: ACCELERATOR AND EXPERIMENTS Collaboration, “LHC Machine”, JINST 3 (2008) S08001, doi:10.1088/1748-0221/3/08/S08001.

[2] R. Aggleton et al., ”An FPGA Based Track Finder for the L1 Trigger of the CMS Experiment at the High Luminosity LHC”, 25 May 2017.

[3] CMS Collaboration, “The CMS experiment at the CERN LHC”, JINST 3 (2008) S08004, doi:10.1088/1748-0221/3/08/S08004.

[4] Davide Cieri, ”DEVELOPMENT OF A LEVEL-1 TRACK AND VERTEX FINDER FOR THE PHASE II CMS EXPERIMENT UPGRADE”, PhD thesis in preparation.

[5] ”The Phase-2 Upgrade of the CMS Trigger, Interim Report to the LHCC”, CMS Collaboration, 12 September 2017.

[6] M. Ester, H.-P. Kriegel, J. Sander, and X. Xu, “A density-based algorithm for discovering clusters in large spatial databases with noise”, 1996.

[7] Michael Hutcheon, "Algorithms for online vertex reconstruction at CMS", 2016.

12 Appendix

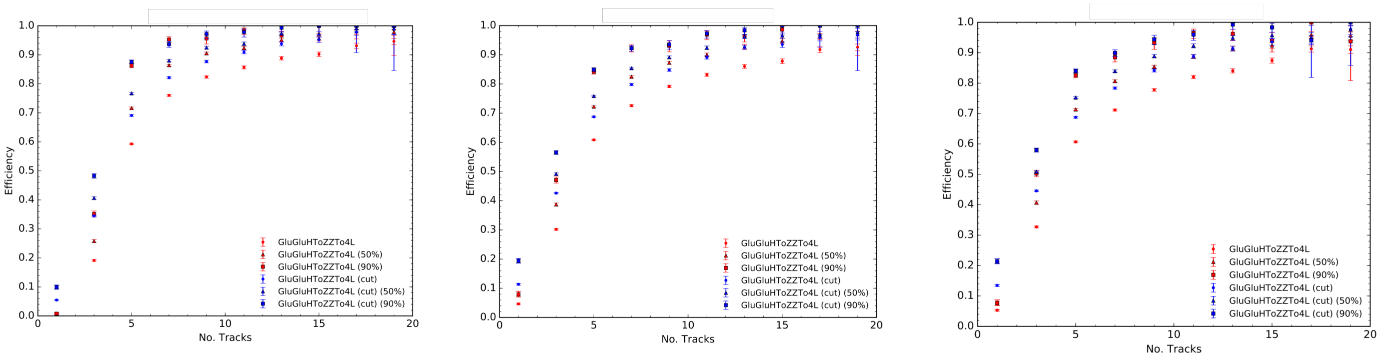

Figure 12: PV reconstruction efficiency of the DBSCAN algorithm for GluGlu $H \to ZZ \to 4L$ with the cuts on 0,50 and 90% of tracks in the barrel and the layers cut at 0, 140 and 200PU.

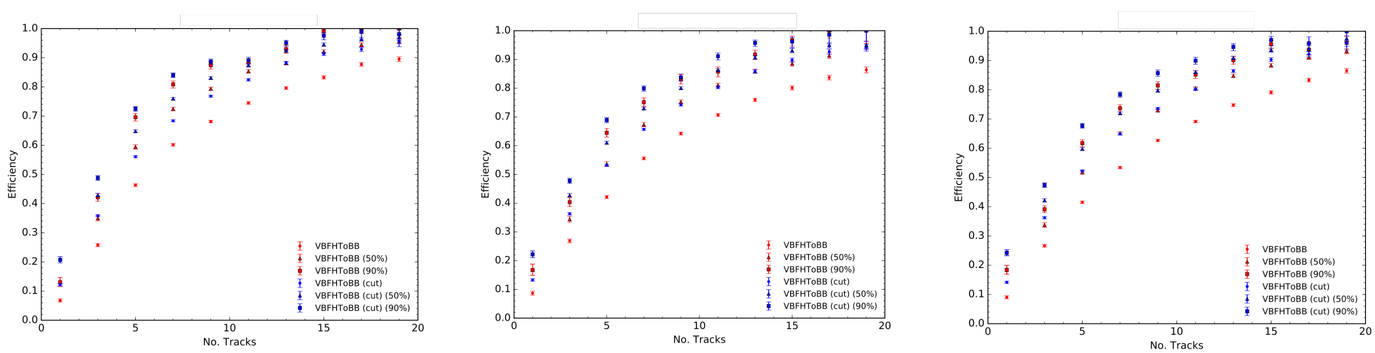

Figure 13: PV reconstruction efficiency of the DBSCAN algorithm for VBF $H \to BB$ with the cuts on 0,50 and 90% of tracks in the barrel and the layers cut at 0, 140 and 200PU.

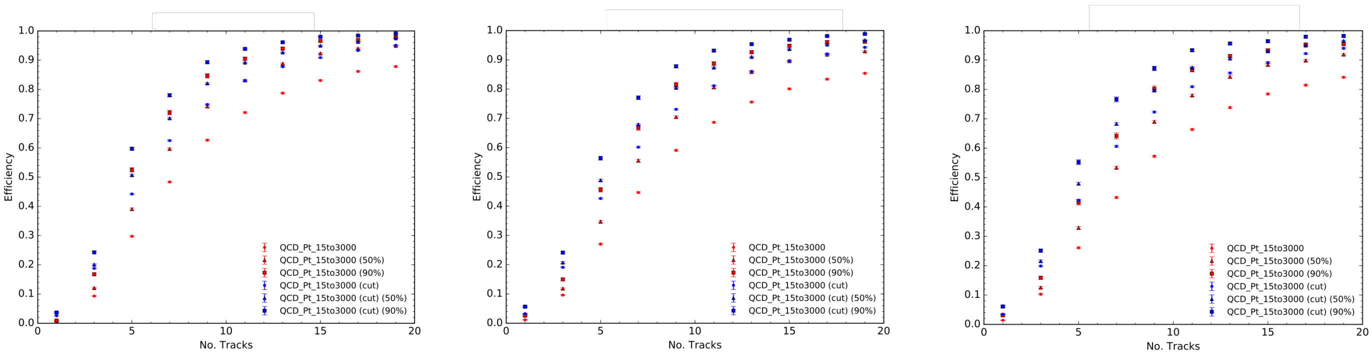

Figure 14: PV reconstruction efficiency of the DBSCAN algorithm for QCD Pt15to3000 with the cuts on 0,50 and 90% of tracks in the barrel and the layers cut at 0, 140 and 200PU.

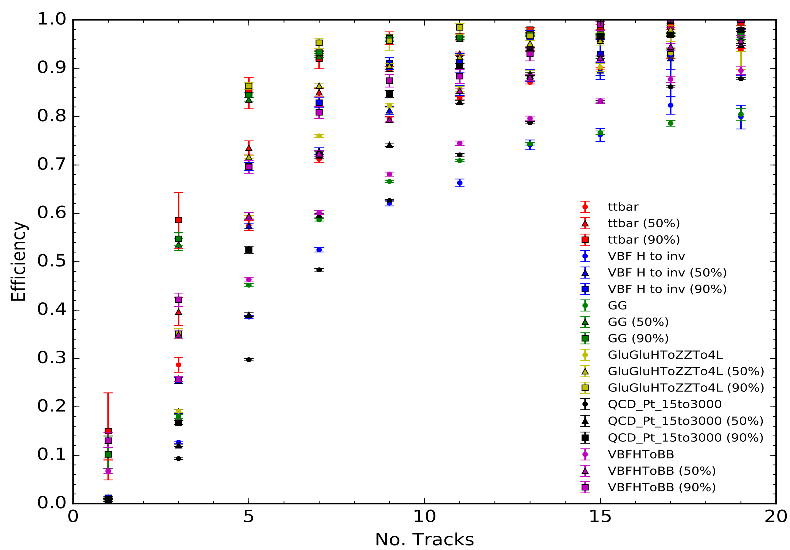

Figure 15: PV reconstruction efficiency of the DBSCAN algorithm for all the considered samples only with the cuts on 0,50 and 90% of tracks inside the barrel at 0 PU.

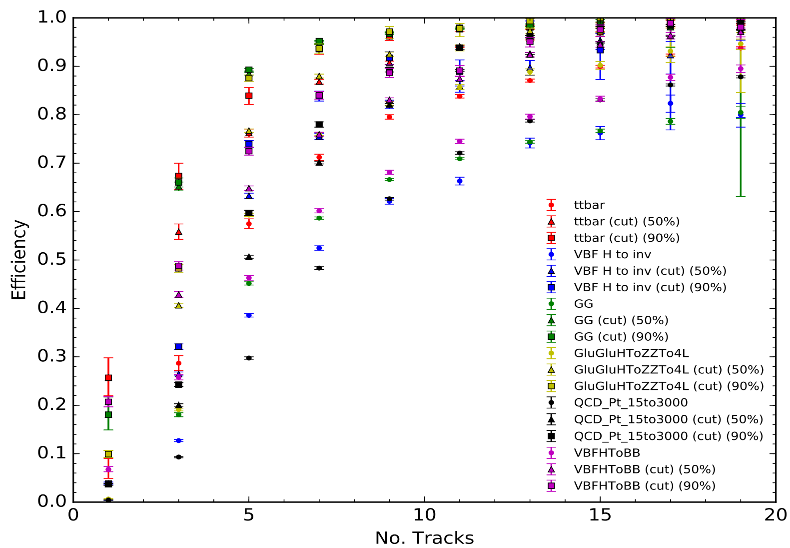

Figure 16: PV reconstruction efficiency of the DBSCAN algorithm for all the considered samples with the cuts on 0,50 and 90% of tracks in the barrel and the layer cuts at 0 PU.